MJSAT

Malaysian Journal of Science and Advanced Technology

journal homepage: https://mjsat.com.my/

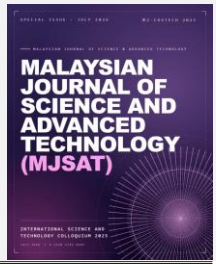

In Silico Docking Analysis of *Phaleria macrocarpa* Fruit Phytochemicals in Inhibiting SARS-CoV-2

Fatin Hannani Mohd Shaharizal, Nurul Zawani Alias*, Ang Lee Sin, and Muhammad Azhar Zulkffle

Fakulti Sains Gunaan, Universiti Teknologi MARA Cawangan Perlis, Kampus Arau, 02600 Arau, Perlis.

KEYWORDS

In silico
Phaleria macrocarpa
SARS-CoV-2 virus

ARTICLE HISTORY

Received 22 November 2025
Available online 21 August 2026

ABSTRACT

SARS-CoV-2 has caused significant global mortality, and while synthetic antivirals are used, their potential side effects highlight the need for safer natural alternatives. *Phaleria macrocarpa* contains antiviral flavonoids but remains underexplored against SARS-CoV-2. This study aimed to identify phytochemicals in *P. macrocarpa* fruit using GC-MS and phytochemical screening, evaluated their antiviral potential to inhibit SARS-CoV-2 through *in silico* docking, and assess their pharmacokinetic properties via SwissADME. Extraction was performed using maceration, followed by screening and GC-MS, which revealed flavonoids, terpenoids, phenolics, sterols, glycosides, and seven compounds, with only squalene showing antiviral activity. Thirteen compounds from databases were further analysed, yielding binding affinities ranging from -5.5 to -8.6 kcal/mol. Among these, sesamin, Mahkoside A, and Mahkoside B exhibited the strongest predicted binding interactions. These findings suggest *P. macrocarpa* phytochemicals may serve as natural alternatives to existing antiviral treatments, warranting further experimental validation.

1. INTRODUCTION

The pandemic that emerged in Wuhan, China, in 2020 has been a devastating event that has caused global chaos, leading to the loss of numerous lives and bringing people together in grief and solidarity. The Ministry of Health Malaysia recently provided an update on the status of SARS-CoV-2, and unfortunately, it appears that the virus is still around. Throughout the years, various methods and medicines have been studied to find the most effective SARS-CoV-2 cure. Among the efforts carried out is to find or develop antivirals that are available from natural or synthetic ingredients. Antiviral agents are specifically designed to combat viral infections, which can range from mild, self-resolving illnesses to severe and potentially deadly diseases. Many vaccines were developed during the year when the virus was widespread.

However, the search for complementary antiviral agents remains important due to the emergence of viral variants and potential limitations of existing therapies. Natural products have gained attention as potential sources of antiviral compounds with fewer side effects. Several plant species, such as *green tea* and *garlic*, have been investigated using *in silico* docking approaches.

Phaleria macrocarpa, locally known as *Mahkota Dewa*, is a species of the Thymelaeaceae family, which is a densely packed evergreen tree that possesses significant botanical and pharmacological potential (Figure 1) [1]. This fruit is abundant in both Malaysia and Indonesia [2] and has been traditionally used for medicinal purposes to treat various health conditions. It exhibits diverse pharmacological activities, including antitumor, anti-hyperglycemic, anti-hyperlipidemic, anti-inflammatory, anti-diarrheal, antioxidant, anti-viral, antibacterial, and anti-fungal and contains compounds such as saponin, tannin, alkaloids, flavanoids, mangiferin, and gallic acid [3]. Radita and Widyarman [4] have shown that the flavonoid component in *P. macrocarpa* extract can inhibit both Gram-positive and Gram-negative bacteria, demonstrating the bioactive potential of this species. In addition, *P. macrocarpa* has shown antiviral activity against various viruses.

While, flavonoids with antiviral properties include quercetin (1), kaempferol (2), myricetin (3), naringenin (4), gallic acid (5), sesamin (6), mangiferin (7), 24-methyl-9,19-

*Corresponding author:
E-mail address: Nurul Zawani Alias < zawani299@uitm.edu.my >.
https://doi.org/10.56532/mjsat.v6iS1.792
2785-8901/

cyclolanost-25-en-3-ol (8), mahkoside A (9), mahkoside B (10), fevidordin A (11) and fevicordin A glucoside (12) as shown in Figure 2. However, *P. macrocarpa* has not yet been analysed for its antiviral potential against SARS-CoV-2. Therefore, this study aims to analyse the *in silico* docking of *P. macrocarpa* phytochemical against SARS-CoV-2 virus.

Fig. 1. a) Whole plant, b) leaves, c) unripe green fruit, d) ripe

red fruit and e) flowers of *Phaleria macrocarpa* (Ahmad et al., 2023)

2. METHODOLOGY

2.1 Materials, chemicals, apparatus and instrument

a) *Materials*: *Phaleria macrocarpa* fruit from Sungai Petani, Kedah.
b) *Chemicals*: Distilled water, 95% Ethanol (C2H5OH), NaOH solution, FeCl3 powder, HCl solution, Concentrated sulphuric acid, Acetic anhydride, Chloroform
c) *Apparatus:* Oven, electric blender, Whatman No. 1 filter paper, rotary evaporator, 250 mL distillation flask, test-tube, test-tube racks, test tube cover, volumetric flask, syringe filter.

2.2 Sample collection and preparation

Phaleria macrocarpa was collected in Kedah. Subsequently, the fruits were washed with water to remove all dirt and unwanted particles. Then, the fruits were dried at 60°C in a hot air oven to remove moisture [5]. The sample was cut into small pieces and ground into coarse powder using an electric blender. The sample was soaked in 95% ethanol for 24 hours at room temperature [4]. After that, it was filtered using Whatman No. 1 filter paper. The extract was diluted by taking 3 mL from the original solution and diluting it with ethanol. This step was repeated twice until the sample became colourless. Lastly, the sample was kept in a closed container.

2.3 Phytochemical screening

The qualitative phytochemical screening of the *P. macrocarpa* fruit extract was conducted for flavonoid, terpenoid, phenolic, sterol and glycoside. These tests were carried out using methods conducted by previous studies [6, 7, 8, 9, 10] with slight modification.

Test for Flavonoid (alkaline reagent test): 50µL of the fruit extract was added with 100µL of sodium hydroxide. Then, a few drops of diluted HCl were added. Intense yellow-brownish colour that turned colourless indicated the presence of flavonoid.

Test for Phenolic (Ferric (III) chloride test): 0.16 g of Ferric (III) chloride was dissolved in 1 ml of distilled water and diluted in 10 ml volumetric flask (0.1 M of FeCl3). Then, 25µL of fruit extract was mixed with 50µL of distilled water in a test tube. Then, a few drops of the Ferric (III) chloride solution were added. Formation of dark green or bluish black colour represent the phenolics.

Test for Sterol: 50µL fruit extract was mixed with 100µL of acetic anhydride. Then, 10µL of concentrated sulfuric acid were added slowly along the test tube. Green or bluish-green colour changes indicated the presence of sterol.

Test for Terpenoid: 50µL of fruit extract was dissolved with 1mL of chloroform. Then, 2-3 drops of acetic anhydride were added into the mixture. Lastly, 2-3 drops of concentrated sulfuric acid were added. Dark green colour changes indicated the presence of terpenoid.

Test for Glycoside: 50µL of fruit extract was dissolved with 500µL of water. Then, a few drops of NaOH were added into the mixture. A yellow colour indicated the presence of glycoside.

2.4 GCMS analysis

The volatile components of the extract were analysed using gas chromatography-mass spectrometry (GC-MS). The injector had an injection volume of 1 µL, a split ratio of 1:40, and a target temperature of 250°C. The GC oven temperature started at 50°C for 20 minutes, increased to 250°C at a rate of 3°C/min, and then rise to 300°C at a rate of 1°C/min. Helium was used as the carrier gas at a constant flow rate of 0.8 mL/min [1]. The MS detector operated in full scan mode, identifying unique peak fragmentation patterns of various metabolites. Metabolite identification was performed by comparing peak spectrum data with standard mass spectra from the spectrometer databases, further validating their identification.

2.5 In silico docking analysis

In silico docking analysis of P. macrocarpa was conducted on all the phytochemical compositions to explore its potential as a therapeutic agent against the SARS-CoV-2 virus.

ADME and other pharmacokinetic properties: The optimal phytochemical compounds in *P. macrocarpa* were chosen based on Lipinski rules of five and antiviral probabilities. According to the Lipinski rule the compound should abide the following criteria (Jr, 2023):

1) *Molecular weight (MW) less than 500 daltons.*
2) *Hydrogen bond acceptor (HBA) less than five.*
3) *Hydrogen bond donor (HBD) less than ten*
4) *High lipolysis (LogP) less than 5*
5) *Molar refractory (MR) 40-130.*

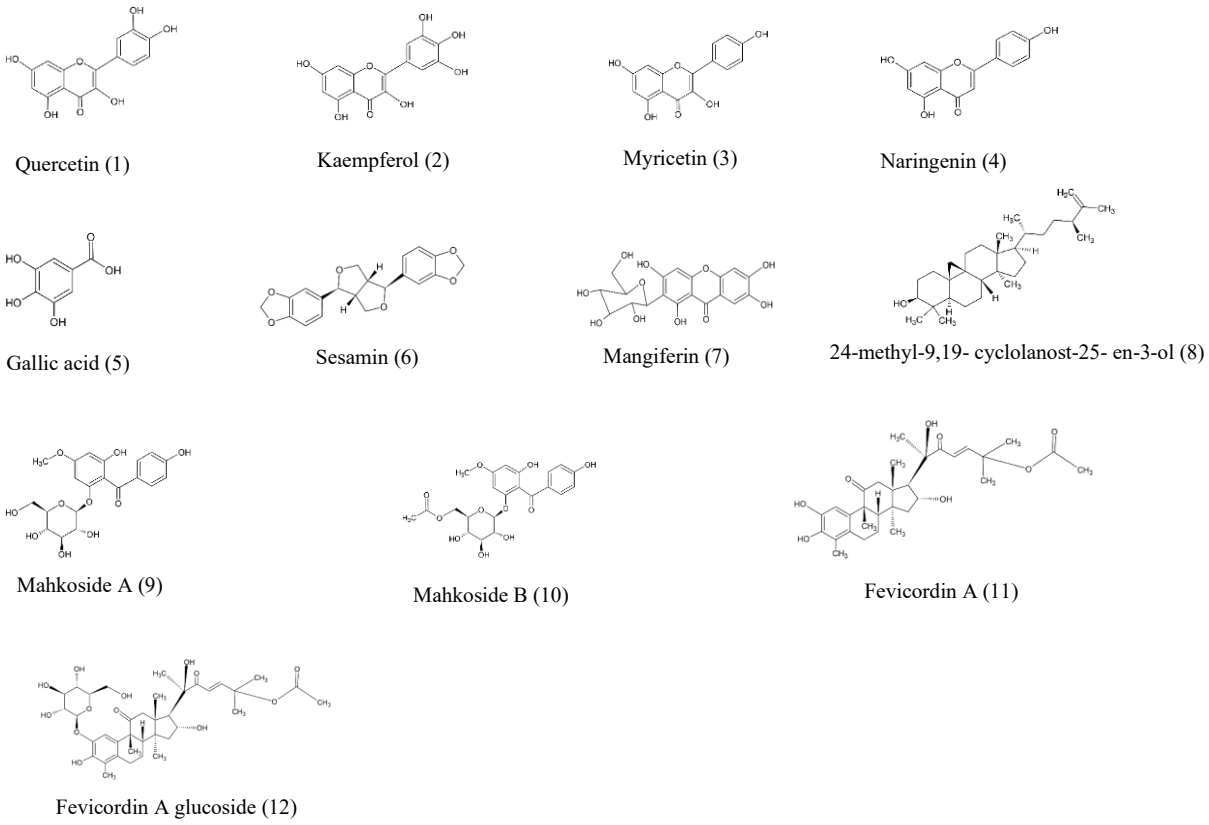

Fig. 2. Structure of flavonoids with antiviral properties

Preparation of ligands and target proteins: The list of phytochemicals present in *P. macrocarpa* was obtained from previously published scientific literature and GCMS analysis. Nirmatrelvir a main ingredient of paxlovid was chosen as positive control. The three-dimensional (3D) conformers of the selected ligands were retrieved from PubChem (http://www.pubchem.ncbi.nlm.nih.gov) database in SDF formats. Ligand's energy-minimization was carried out using PyRx and converted to PDBQT format.

Similarly, the 3D structures of proteins determined using a biophysical technique such as X-ray crystallography or NMR spectroscopy are openly available in protein data bank were retrieved (www.rcsb.org). 3-chymotrypsin-like protease (3CLpro) or known as Mpro viral target was considered for docking studies

The downloaded 3D structures were checked for the presence of water molecules, complex molecules, ions and ligands of the protein and were removed using Biovia Discovery Studio 2021. Each protein was added a polar hydrogen bond and sterile protein was utilized for docking using PyRx.

Antiviral probability prediction: Bioactive prediction of antiviral potential was analysed using the PASS Online web: (https://www.way2drug.com/passonline/predict.php). The category of predictions sought was antiviral. The parameter in this analysis is the probability to be active (Pa) and the probability to be inactive (Pi) value. The potential activity standard used are Pa score >0.3 and Pa>Pi.

Active site prediction and molecular docking: Sterile protein 3D structure was uploaded to DoGSiteScorer online tool in PDB format to assess predicted mostly likely suitable binding pockets based on durability by considering drug score values [11]. DoGSiteScorer is a grid- based method that applies a difference of Gaussian filter to detect potential binding pockets solely based on protein structure [12]. The pocket structure with the highest drug score pocket was downloaded and visualized in PyMoL to identify the exact residue. The optimized ligand and protein were subjected to molecular docking with the aid of the Auto Dock Vina function based on the predicted binding pocket, the grid box was set with centre values of -10.7106, 12.4187, 68.8194 (XYZ coordinates) for (6LU7) 3CLpro [13]. The output file of docking was obtained with an exhaustiveness value of 8 and 9 models respective to binding affinity. The best-ranked pose with the lowest binding energy was selected for further analysis. Prior to docking, ligand structures were energy-minimized using the Universal Force Field (UFF) to relieve steric clashes.

3. Results and Discussions

3.1 Confirmation Species and GC-MS Analysis

The species has been confirmed, and it has been verified that the species used is *Phaleria macrocarpa* or Mahkota Dewa. The confirmation was completed by sending the plant to UKM, and the voucher number ID137/2024 was obtained.

After subjecting *P. macrocarpa* fruit extract to GC-MS analysis a total of 7 peaks with more than 80% of quality were identified. As shown in Table 1, the GC-MS spectrum confirmed the presence of various components with varying retention times. Individual compounds were identified by comparing their mass-spectral database with NIST/EPA/NIH version 2.0. The compounds identified are phenol, n-hexadecanoic acid, squalene, phenol, 2,4-bis(1,1-dimethylethyl)-, 5-hydroxymethylfurfural, 1,4,7,10,13,16-hexaoxacyclooctadecane and oleic acid.

Based on the GC-MS analysis, the compounds with antiviral properties were not detected. This outcome could be attributed to several potential factors, such as incomplete reaction, degradation of the compound during analysis, insufficient sensitivity of the instrument, or improper sample preparation. However, one compound was found to potentially exhibit antiviral properties which is squalene [14]. Research findings, including a clinical trial involving COVID-19 patients, suggest that squalene may have the potential but, the study does not provide conclusive evidence regarding its efficacy as a treatment, and it state that further studies are required to confirm the results. In a study, squalene functions primarily as a vaccine adjuvant. It is used to enhance the immune response to vaccines, improving their efficacy [15]. Squalene belongs to the triterpenes class, which means it is under terpenoids [15]. The results from the phytochemical tests further support this classification, as the terpenoid test also yielded a positive outcome, confirming the presence of squalene.

3.2 Phytochemical Screening Test

The phytochemical screening tests were conducted to detect the presence of flavonoids, terpenoids, phenolics, sterols and glycoside in the sample. Specific qualitative methods were employed for each class, such as the alkaline reagent test for flavonoids, the Liebermann-Burchard test for terpenoids, the ferric chloride test for phenolics, the acetic anhydride test for sterol and the NaOH test for glycoside. The phytochemical test shown in Table 2 includes visual observations of colour changes that indicate the presence of these compounds. While the visual nature of these tests offers quick and accessible results, certain limitations, such as subjective interpretation of colour changes, were noted. Overall, the findings align with the research objectives by providing a preliminary assessment of the bioactive potential of the sample.

The initial colour of the sample was caramel brown. Upon performing the flavonoid test, the brown colour of the extract faded to a light yellow. According to previous studies, the expected outcome of this test is a colourless solution, which indicates a significant flavonoid content [6]. However, in this case, the result did not turn colourless, likely due to the low flavonoid content in the sample. During the test, NaOH was added first, causing the appearance of a light-yellow colour. Interestingly, as a drop of NaOH fell into the sample, a transient pink colour briefly appeared before disappearing, resembling the behaviour seen during titration when a drop of reagent momentarily reacted in the solution. This may be due to the stability of the compound in an alkaline environment or an unstable pH reaction in solution [16]. Afterward, upon the addition of HCl, the yellow colour became paler but did not fade to a colourless state, further suggesting a negative result or assumed to be a lower concentration of flavonoids in the sample.

Table 1. Phytochemical profile of *Phaleria macrocarpa* fruits extract obtained via GC-MS analysis

Name of compound	Formula	MW (g/mol)	Mass fragments m/z	Peak area (%)	RT (min)	Quality	Activity	Reference
Phenol	C_6H_6O	94.11 g/mol	69.10, 81.10, 45.10, 41.10, 89.10	0.7651	8.2631	90	Antioxidant	Ferreira et al., (2018)
Phenol, 2,4-bis(1,1-dimethylethyl)-	$C_{14}H_{22}O$	206.32 g/mol	41.10, 45.10, 57.10, 43.10, 191.20	3.0494	9.6336	96	Antioxidant and cytotoxic	Mostofa et al., (2023)
5-Hydroxymethylfurfural	$C_6H_6O_3$	126.11 g/mol	45.10, 41.10, 97.00, 43.00, 39.10	0.9814	10.5277	80	Antioxidant and antiproliferative	Zhao et al., (2013)
1,4,7,10,13,16-Hexaoxacyclooctadecane	$C_{12}H_{24}O_6$	264.31 g/mol	45.10, 43.10, 44.00, 89.10, 73.10	0.1152	10.6042	86	Unknown	Pubchem
n-Hexadecanoic acid	$C_{16}H_{32}O_2$	256.42 g/mol	73.10, 43.10, 60.10, 41.10, 45.10	17.7844	12.0629	99	Antibacterial and Antioxidant	Purushotham an et al., (2024)
Squalene	$C_{30}H_{50}$	410.7 g/mol	69.10, 81.10, 45.10, 41.10, 89.10	17.6263	13.057	91	Antiviral	Ebrahimi et al., (2022)
Oleic Acid	$C_{18}H_{34}O_2$	282.5 g/mol	45.10, 55.10, 43.10, 41.10, 69.10	11.5271	13.3158	92	Anti-Inflammatory	María et al., (2022)

Table 2. Qualitative phytochemical analysis of *Phaleria macocarpa* fruit extract

Phytochemical Constituents	Phytochemical test	Result
Flavonoid	Alkaline reagent test	+
Terpenoid	Liebermann-Burchard	+
Phenolic	Ferric chloride	+
Sterol	Acetic anhydride + concentrated sulfuric acid	+
Glycoside	NaOH	+

The Liebermann-Burchard test was conducted to determine the presence of terpenoids in the sample. The results showed the formation of two layers, which consisted of a top layer with a slight greenish tinge and a bottom layer is colourless. According to previous studies, the expected outcome for a strong positive result is a dark green solution [7]. However, the observed result indicates a positive but weak reaction, suggesting the presence of terpenoids in lower concentrations or partial reactivity. During the test, the colour changes and layer forms when sulfuric acid is added. Layers may form at this step due to density differences between these solvents.

Next is the phenolic test, which was conducted using a ferric chloride reagent. The test showed a positive result. Previous studies have shown that dark green colour is typically observed to indicate the presence of phenolic compounds [8]. Similarly, the test resulted in the formation of a dark green colour. This indicates the presence of phenolic compounds in the sample, which reacted strongly with ferric chloride, confirming a significant concentration of phenolic substances.

Then, a test to indicate the presence of sterol. From the observation, the brown colour of the extract transformed into a moss-green colour, which is consistent with the expected result. This positive outcome further confirms the presence of sterols in the sample [9]. Initially, when acetic anhydride was added, the colour remained unchanged, but once concentrated sulfuric acid was added, a colour change occurred, as shown in the table. Finally, NaOH was added to test the presence of glycosides. The observations showed a yellow coloration, confirming the presence of glycosides in the sample [10]. This result aligns with the expected outcome.

3.3 Physicochemical and drug-likeness properties

Table 3 presents the drug-likeness and physicochemical properties of the compounds, as predicted by SwissADME software. For a compound to be considered as a potential drug, several criteria under Lipinski's rule must be met. The first is that molecular weight must be <500. This is because lower molecular weight tends to pass through the cell membrane easily since it is light and have optimal binding interaction with biological targets in molecular docking studies [17]. The second is that the log of skin permeability (log P) value should be <5, which serves as a benchmark for how well the drug is soluble and permeable [18]. The third criterion is that the hydrogen bond donor value must be <5. Hydrogen bond donors are essential for target-ligand interactions, enhancing binding affinity [19]. The fourth criterion is hydrogen bond acceptors, which should be <10. If the value is higher, absorption and distribution in the body will be difficult [20].

Lastly, the molar refraction value must be between 40-130 for optimal absorption and oral bioavailability. A compound that adheres to Lipinski's rule must comply with at least 4 out of the 5 rules [21]. These conditions include having <5 H-bond donors, <10 H-bond acceptors, a molecular weight <500 g/mol, and a Log p value less than 5. If a compound violates two or more of Lipinski's rules, it is classified as orally inactive [22].

Based on the properties obtained, only kaempferol, naringenin, sesamin and paxlovid fully meet the criteria of Lipinski's rule and are considered orally active [20]. Compounds that can still be considered include quercetin, myricetin, gallic acid, and squalene, as they comply with 4 out of 5 criteria. Compounds other than these are considered orally inactive. Nevertheless, squalene does not have a log P value available, likely due to a lack of data in the SwissADME database.

All compounds are referenced based on Paxlovid as a benchmark for their potential to act as inhibitors. If the positive predictions exceed the reference compound, the higher the potential and the better the compound as inhibitor. As shown in the Table 4, paxlovid have a high GI absorption, have Pgp substrate, and have a CYP3A4 inhibitor. P-glycoprotein (Pgp) substrate is a measure of a compound's ability to penetrate cellular organelles which mean the compound can move freely within the circulatory system [23]. While all the CYP code is refer to the Cytochrome P450 enzymes. This is to know the bioavailability or how far and how quickly a drug can be absorbed into the bloodstream when taken orally or though other method and the clearance, the body's ability to remove the drug from the system, either through the liver or the kidneys [24, 23]. Each CYP inhibitor has its specific function, but the foundation remains as explained before.

As depicted in the Table 4, compound that is most prominent is sesamin. It has a high GI absorption, have Blood-brain barrier (BBB) permeant, CYP2C19 inhibitor, CYP2D6 inhibitor and CYP3A4 inhibitor. The second-best compound after sesamin is naringenin. Naringenin have almost the same pharmacokinetic prediction as paxlovid which is a high GI absorption, Pgp substrate and CYP3A4 inhibitor but with the addition of CYP1A2 inhibitor. Then, quercetin and kaempferol also a good compound since both have the same prediction, which is high GI absorption, have CYP1A2 inhibitor, CYP2D6 inhibitor and CYP3A4 inhibitor. Fevicordin A, a compound rarely discussed and uniquely specific to the species P. macrocarpa, demonstrate a slight potential to act as an inhibitor. Based on the pharmacokinetic prediction obtained, it has a low GI absorption, however, it has a Pgp substrate, and CYP3A4.

Table 3. Physicochemical and drug-likeness properties based on Lipinski's rule for phytoconstituents of *Phaleria macrocarpa* and Paxlovid

Compound	MW <500 D	Log P < 5	HBD < 5	HBA < 10	Molar refractory 40-130	Lipinski's Rule
Mahkoside A	422.38 g/mol	0.06	6	10	101.00	Yes, 2 Violation
Mahkoside B	464.42 g/mol	0.38	5	11	110.74	Yes, 2 Violation
Fevicordin A	528.63 g/mol	3.31	4	8	143.22	Yes, 2 Violation
Fevicordin A glucoside	676.75 g/mol	1.33	7	13	170.66	Yes, 4 Violation
Quercetin	302.24 g/mol	1.23	5	7	78.03	Yes, 1 Violation
Kaempferol	286.24 g/mol	1.58	4	6	76.01	No, 0 Violation
Myricetin	318.24 g/mol	0.79	6	8	80.06	Yes, 1 Violation
Naringenin	272.25 g/mol	1.84	3	5	71.57	No, 0 Violation
Gallic acid	170.12 g/mol	0.21	4	5	39.47	Yes, 1 Violation
Sesamin	354.35 g/mol	2.79	0	6	90.00	No, 0 Violation
Mangiferin	422.34 g/mol	0.77	8	11	100.70	Yes, 2 Violation
24-methyl-9,19-cyclolanost-25- en-3-ol	440.74 g/mol	7.82	1	1	139.95	Yes, 2 Violation
Squalene	410.72 g/mol	-	0	0	143.48	Yes, 1 Violation
Paxlovid	499.53 g/mol	1.89	3	8	125.68	No, 0 Violation

Table 4. Pharmacokinetics prediction results for phytoconstituent of *Phaleria macrocarpa* and Paxlovid

Compound	GI Absorption	BBB Permeant	Pgp Substrate	CYP1A2 Inhibitor	CYP2C19 Inhibitor	CYP2C9 Inhibitor	CYP2D6 Inhibitor	CYP3A4 Inhibitor
Mahkoside A	Low	No	Yes	No	No	No	No	No
Mahkoside B	Low	No	Yes	No	No	No	No	No
Fevicordin A	Low	No	Yes	No	No	No	No	Yes
Fevicordin A glucoside	Low	No	Yes	No	No	No	No	No
Quercetin	High	No	No	Yes	No	No	Yes	Yes
Kaempferol	High	No	No	Yes	No	No	Yes	Yes
Myricetin	Low	No	No	Yes	No	No	No	Yes
Naringenin	High	No	Yes	Yes	No	No	No	Yes
Gallic acid	High	No	No	No	No	No	No	Yes
Sesamin	High	Yes	No	No	Yes	No	Yes	Yes
Mangiferin	Low	No	No	No	No	No	No	No
24-methyl-9,19-cyclolanost-25-en-3-ol	Low	No	No	No	No	No	No	No
Squalene	Low	No	No	No	No	No	No	No
Paxlovid	High	No	Yes	No	No	No	No	Yes

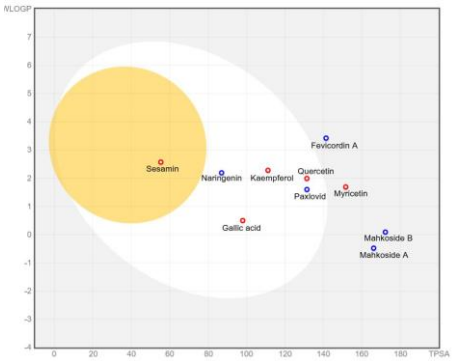

Fig. 3. BOILED-Egg model for the test compound

Figure 3 shows BOILED-Egg generated by the SwissADME to predict a molecule's ability to penetrate the Blood-Brain Barrier (BBB) and its absorption through the gastrointestinal (GI) tract. This is just the same from the table 4 but being visualized to interpret the potential of a compound quickly. The points within the white ellipse indicate compounds that are likely to be passively absorbed through the gastrointestinal tract. Quercetin, kaempferol, naringenin, gallic acid and paxlovid, are found in the white part. Molecules outside the egg or in the grey zone are molecules not predicted to be well absorbed nor BBB permeant. There are 4 molecules in this part which are molecule Mahkoside A, Mahkoside B, Fevicordin A and myricetin. The points in the yellow ellipse or the yolk are for compounds with a high probability to permeate through the BBB to reach the central nervous system (CNS). Only one compound is included in this part which is sesamin.

Points shown in blue represent molecules expected to be substrates of P- glycoprotein (PGP+) and are therefore actively transported out of the brain or into the gastrointestinal tract. The compound with this indicator gives a good property because it gives a protection against toxicity and prevents unwanted accumulation into the central nervous system [25, 26]. If predicted to be non-substrates of P-glycoprotein (PGP-), the corresponding points are shown in red. There are four molecules (fevicordin A glucoside, mangiferin, 24-methyl-9,19- cyclolanost-25-en-3-ol and squalene) out of the range of the BOILED-Egg model. Overall prediction on SwissADME, sesamin is the best compound that can act as an inhibitor.

3.4 In silico docking analysis

An automated docking program, specifically the AutoDock Vina package within PyRx 8.0, was utilized to explore the intricate intermolecular interactions between the ligand and the target protein (SARS-CoV-2 Mpro). It conducts grid-based ligand docking that incorporates energetics and investigates the advantageous interactions between one or more smaller ligand molecules and a larger receptor molecule, which is usually a protein. The three-dimensional structure of the target was sourced from the Protein Data Bank (PDB) entry 6LU7. The receptor preparation involved removing water molecules that were not linked to the active sites, as well as restoring the native conformation and adding hydrogen atoms. The compounds derived from *P. macrocarpa* were then docked into the active site of the SARS-CoV- 2 main protease (Mpro). The most reliable way to assess the precision of a docking process is to

Table 5. Docking score of thirteen phytochemicals from P. macrocarpa and Paxlovid with SARS CoV-2 main protease

Ligand	Binding Affinity
Mahkoside A	-7.4
Mahkoside B	-7.5
Fevicordin A	-7
Fevicordin A glucoside	-7.3
Quercetin	-7.3
Kaempferol	-7.7
Myricetin	-7.4
Naringenin	-7.7
Gallic acid	-5.5
Sesamin	-7.8
Mangiferin	-8.6
24-methyl-9,19- cyclolanost-25- en-3-ol	-6
Squalene	-6
Paxlovid	-7.4

examine how well the object scoring function predicts the lowest energy conformation (binding pose). The more negative the binding affinity between the ligand and receptor, the stronger the interaction, which generally indicates a better compound [11]. Paxlovid is an oral antiviral medication that has been shown to inhibit SARS- CoV-2 and various other RNA viruses [27]. Therefore, it was used in this study as a reference molecule for docking against SARS-CoV-2 main protease.

The binding energies of thirteen phytochemicals from *P. macrocarpa* and Paxlovid against SARS CoV-2 main protease (Mpro) are summarized in Table 5. It is revealed that phytochemicals in *P. macrocarpa* exhibited lower binding energy compared to the reference molecule, Paxlovid. Lower binding energy indicates the higher binding affinity of the molecules to target receptors [28]. The range of binding energy with SARS- CoV-2 main protease towards phytochemicals of *Phaleria macrocarpa* were from -8.6 to -5.5 kcal mol-1, which was better and significant than the binding energy of paxlovid (-7.4 kcal mol-1). Based on the docking analysis, mangiferin produce the highest binding affinity. According to previous studies, mangiferin indeed possesses antiviral properties [29]. Thus, the compounds (Mahkoside A and Mahkoside B) specific to this species have received special attention as they have not yet been docked, and their binding energies are comparable to that of Paxlovid.

The molecular interactions of phytochemicals from *P. macrocarpa* and Paxlovid against main protease target site were analysed using BIOVIA and superimposition images. The visualization of molecular interactions between mahkoside A with Mpro through BIOVIA showed that mahkoside A interacted with MET49A and CYS145A through Pi-alkyl and alkyl contacts (Figure 15) Mahkoside A formed carbon-hydrogen bonds with residues GLN189A and ASP187A that maintains a strong affinity with the target protein. There's also conventional hydrogen bond interaction with GLU166A, THR190A and LEU141A. Among 7 residues, interactions with 2 of the residues matches with the reference molecule (Figure 15). Mahkoside B interacted with MET49A, HIS41A and CYS145A through Pi-alkyl and alkyl contacts (Figure 16). It formed carbon-hydrogen bonds with residues GLN189A and ASP187A. The conventional hydrogen bond is observed with SER144A and ARG188A and there is a Pi-sulfur interaction with MET165A. Out of the interactions with 8 of the residues, 2 matches of the drug Paxlovid. Fevicordin A interacted with ALA191A through Pi-alkyl contacts (Figure 13). The conventional hydrogen bond interacts with SER144A,

GLN189A and CYS145A. Among interactions with 4 of the residues, 1 of it matches with that to the drug Paxlovid (Figure 13). Fevicordin A glucoside interacted with PRO168A through Pi-alkyl and alkyl contacts (Figure 14). The conventional hydrogen bond interacts with ASN142A and GLN189A. Among interactions with 3 of the residues, 2 of it matches with that to the drug Paxlovid. Quercetin interacted with CYS145A through Pi-alkyl (Figure 9). It formed unfavourable donor-donor and unfavourable acceptor-acceptor with residues HIS163A. The conventional hydrogen bond interacts with SER144A, LEU141A andARG188A and the Pi-sulfur interact with MET165A. Among interactions with 6 of the residues, 2 of it matches with that to the drug paxlovid. Kaempferol interacted with MET49A through Pi-alkyl contacts (Figure 10). It formed Pi-donor hydrogen bonds with residues GLU166A. The conventional hydrogen bond interacts with GLN189A and ASP187A and the Pi-sulfur interact with MET165A and CYS145A. Kaempferol have Pi-pi stacked interaction with HIS41A. Among interactions with 7 of the residues, 2 of it matches with that to the drug paxlovid. Myricetin interacted with MET165A, LEU141A, GLY143A and CYS145A through conventional hydrogen bond (Figure 5). At the same time CYS145A interact with Pi-alkyl and MET165A with Pi-sulfur. It formed carbon hydrogen bonds with residues GLN189A. Myricetin formed unfavourable donor-donor with residues SER144A. Among interactions with 6 of the residues, 2 of it matches with that to the drug paxlovid. Naringenin interacted with ASP187A, GLU166A and SER144A through conventional hydrogen bond (Figure 8). It formed carbon hydrogen bonds with residues ARG188A. Naringenin formed Pi-alkyl with residues MET49A and CYS145A. The interaction Pi-sulfur and Pi-pi stacked formed at MET165A and HIS41A respectively. Among interactions with 8 of the residues, 2 of it matches with that to the drug Paxlovid. Gallic acid interacted with and CYS145A through Pi-alkyl contacts (Figure 4). The conventional hydrogen bond interacts with SER144A, HIS163A, GLU166A and GLN189A. There's unfavourable donor-donor interaction with GLY143A. Among interactions with 6 of the residues, 4 of it matches with that to the drug Paxlovid. Sesamin formed carbon hydrogen bonds with residues THR190A and GLU166A (Figure 6). It interacted with PRO168A through Pi-sigma. The interaction Pi-alkyl formed at MET165A. Sesamin have amide-Pi stacked interaction with LEU167A. Among interactions with 5 of the residues, 1 of it matches with that to the drug Paxlovid. Mangiferin interacted with MET165A through Pi-alkyl (Figure 11). It formed unfavourable acceptor-acceptor with residues LEU141A. The conventional hydrogen bond interacts with THR190A, HIS164A, SER144A and ASN142A. Among interactions with 6 of the residues, 1 of it matches with that to the drug Paxlovid. 24- Methyl-9,19-cyclolanost-25-en-3-ol only have one alkyl interaction with PRO168A. This interaction does not match with the drug paxlovid (Figure 7). Squalene interacted with PRO168A, CYS145A, MET165A, MET49A and HIS41A through Pi-alkyl and alkyl contact. Among interactions with 5 of the residues, none of them matches with that to the drug Paxlovid.

3.5 Structure activity relationship

Structure activity relationship refers to the study of how changes in the chemical structure of a molecule influence its biological activity. Aromatic ring and hydrogen bond are often study in ligand-binding affinity since the presence derivatives correlates with the antiviral activity [30]. Aromatic ring is crucial because it can form π-π interactions that beneficial for binding to viral target [31]. Based on the Table 5, mangiferin has the highest binding affinity value which is -8.6. The structure of mangiferin contains an aromatic ring with many hydroxyl (-OH) groups attached which may contribute to its predicted binding affinity. This suggests a favourable binding interaction in the *in silico* docking analysis. The second highest binding affinity value is -7.8 for sesamin. The structure show that it does not have -OH group, however the high value of binding affinity may contribute by the aromatic rings. The lowest affinity binding value is -5.5 for gallic acid. The gallic acid has both aromatic ring and -OH group, however it produces a low affinity binding value. This might be due to the structural consideration and interaction forces [32]. The presence of multiple hydroxyl groups leads to intramolecular hydrogen bonding that hinder its ability to interact effectively with binding sites on target molecules. Then, the binding interactions are primarily driven by weak forces such as van der Waals forces and hydrogen bonds, which may not be sufficient for strong binding affinity [32].

In this study, the special compounds that stand out from *P. macrocarpa* are Mahkoside A, Mahkoside B, sesamin and squalene. Squalene is studied due to its presence in the GC-MS analysis. [14] reported the potential of squalene against SARS-CoV-2 via clinical study. However, *in silico* docking shows that, this compound does not meet the Lipinski's rule and the pharmacokinetics prediction. In addition, it has a low binding affinity of -6 kcal/mol. The structure of the compound also lacks -OH group and aromatic rings, which limits interaction with main protease. Therefore, squalene did not show strong predicted inhibitory potential in the present in silico docking analysis. Mahkoside A and Mahkoside B showed strong predicted binding affinities; however, their SwissADME profiles suggest unfavourable pharmacokinetic properties. This can be seen in the result that it does not obey the lipinski's rule with 2 violation which is on the hydrogen bond acceptor (HBA) and hydrogen bond donor (HBD) for both compounds. Plus, it also has low GI absorption. For a compound to be a potential drug, these factors must be considered, as unfavourable pharmacokinetic properties may limit their drug-likeness. Hence, sesamin emerged as the most promising candidate based on the *in silico* analyses. Its SwissADME showing no violations of Lipinski's rule, and its aromatic structure may contribute to favourable molecular interactions. The pharmacokinetics prediction results also shows that sesamin has high GI absorption and is predicted to have blood–brain barrier permeability. Nevertheless, these findings remain predictive, and further validation through *in vitro* and *in vivo* studies is required.

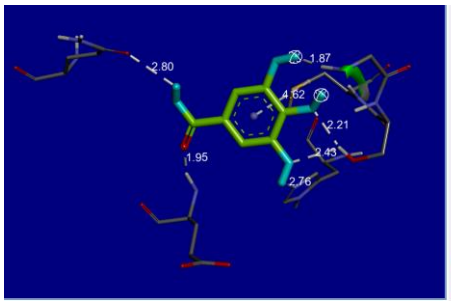

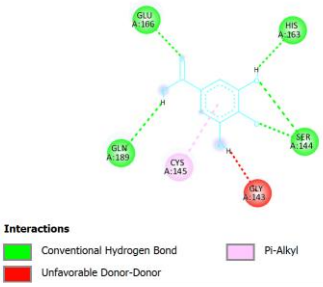

Gallic acid (a)

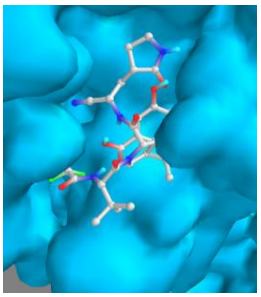

Super imposition of paxlovid and gallic acid (a)

Fig. 4. 2D and 3D visualization of molecular interactions between SARS-CoV- 2 main protease and gallic acid

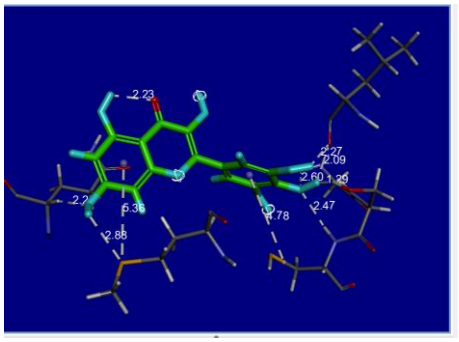

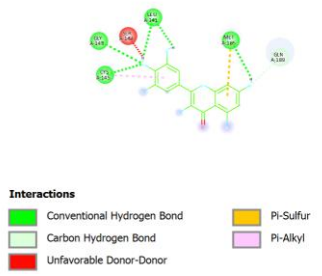

Myricetin (b)

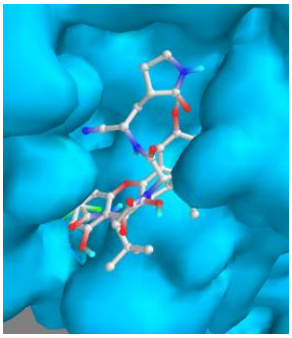

Super imposition of paxlovid and myricetin (b)

Fig. 5. 2D and 3D visualization of molecular interactions between SARS-CoV- 2 main protease and myricetin

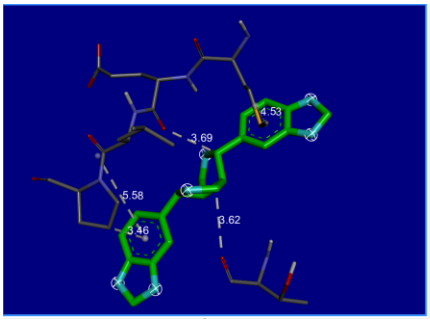

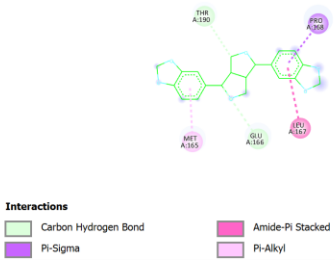

Sesamin (c)

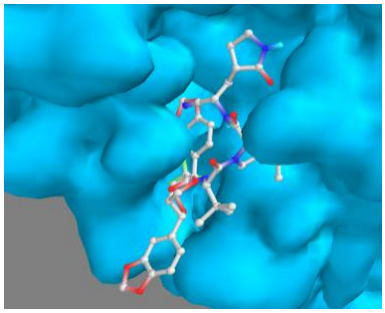

Super imposition of paxlovid and sesamin (c)

Fig. 6. 2D and 3D visualization of molecular interactions between SARS-CoV- 2 main protease and sesamin

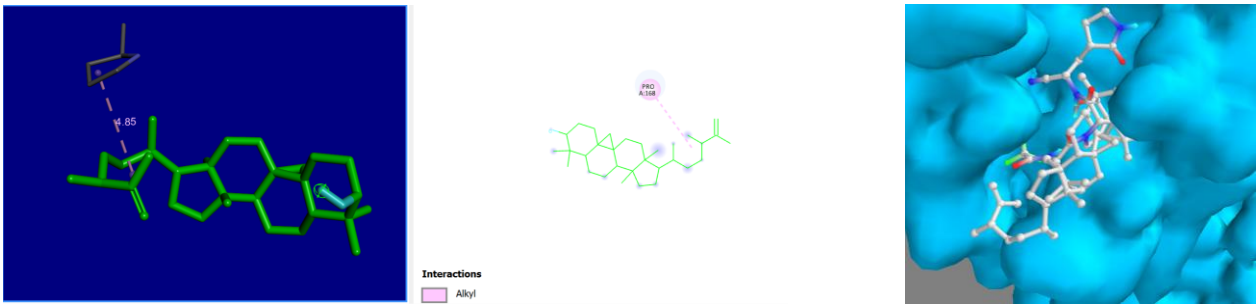

24-Methyl-9,19-cyclolanost-25-en-3-ol

Super imposition of paxlovid and 24-Methyl-9,19-cyclolanost-25-en- 3-ol (d)

Fig. 7. 2D and 3D visualization of molecular interactions between SARS-CoV- 2 main protease and 24-Methyl-9,19-cyclolanost-25-en-3-ol

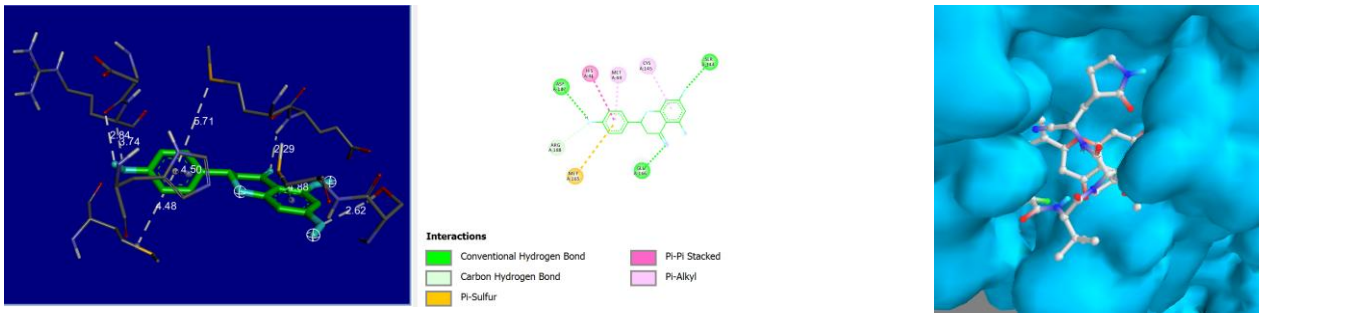

Naringenin (e)

Super imposition of paxlovid and naringenin (e)

Fig. 8. 2D and 3D visualization of molecular interactions between SARS-CoV- 2 main protease and naringenin

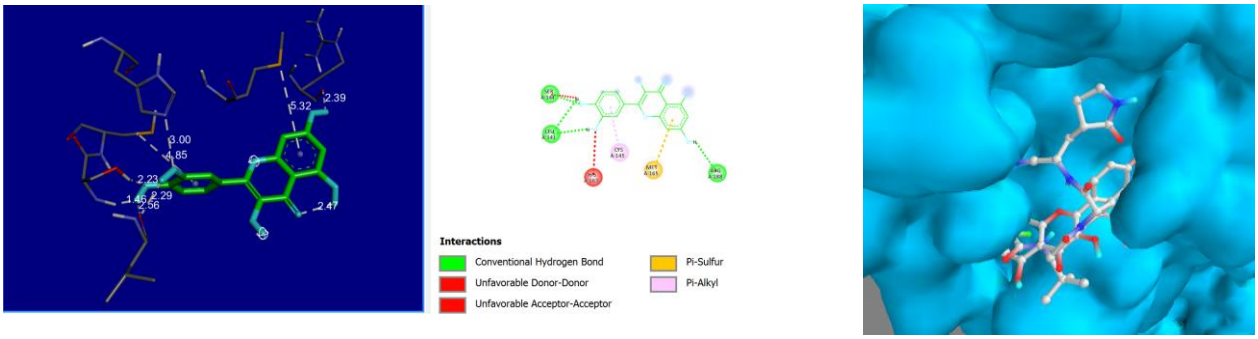

Quercetin (f)

Super imposition of paxlovid and quercetin (f)

Fig. 9. 2D and 3D visualization of molecular interactions between SARS-CoV- 2 main protease and quercetin

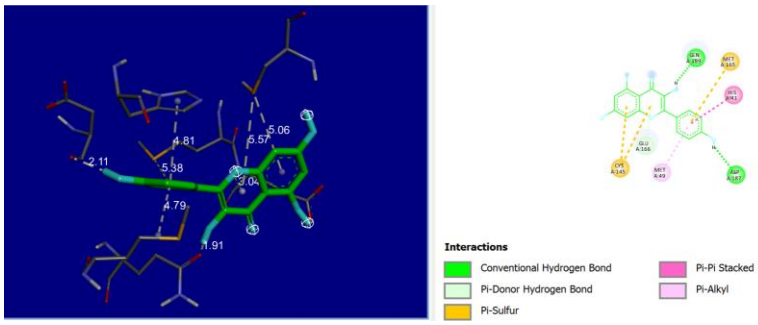

Kaempferol (g)

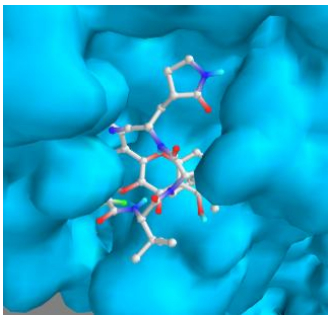

Super imposition of paxlovid and kaempferol (g)

Fig. 10. 2D and 3D visualization of molecular interactions between SARS-CoV- 2 main protease and kaempferol

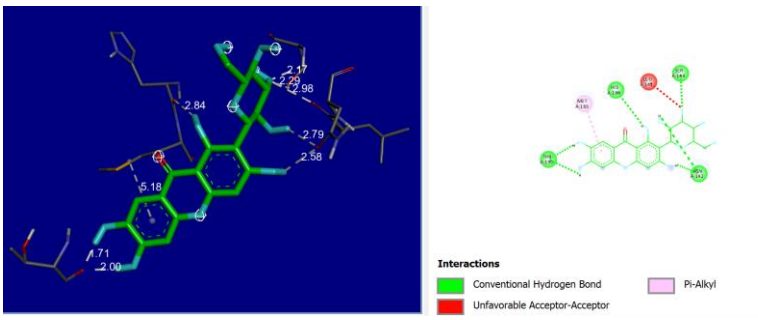

Mangiferin (h)

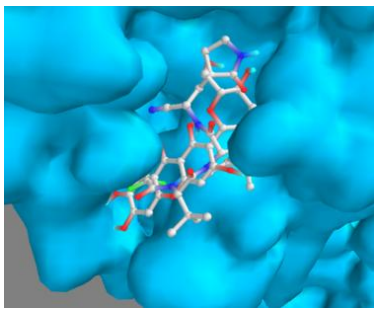

Super imposition of paxlovid and mangiferin (h)

Fig. 11. 2D and 3D visualization of molecular interactions between SARS-CoV- 2 main protease and mangiferin

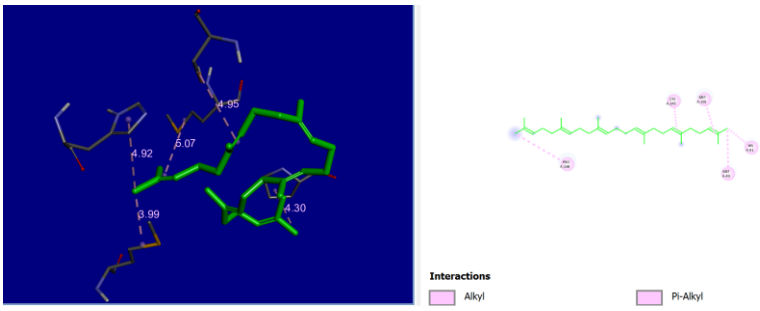

Squalene (i)

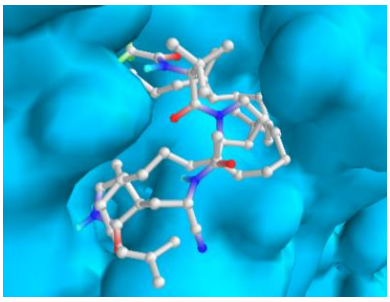

Super imposition of paxlovid and squalene (i)

Fig. 12. 2D and 3D visualization of molecular interactions between SARS- CoV-2 main protease and squalene

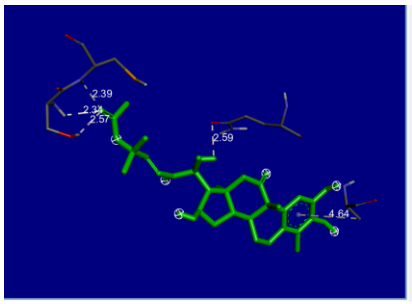

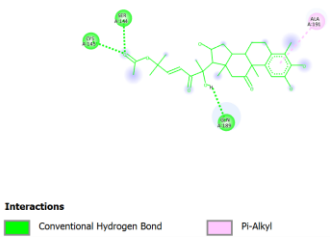

Fevicordin A (j)

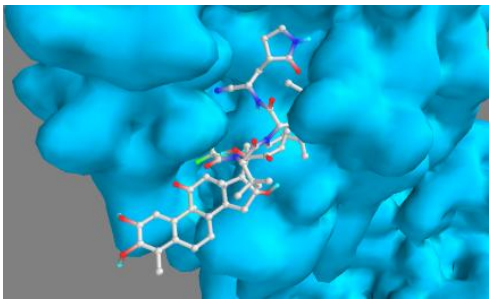

Super imposition of paxlovid and fevicordin A (j)

Fig. 13. 2D and 3D visualization of molecular interactions between SARS- CoV-2 main protease and Fevicordin A

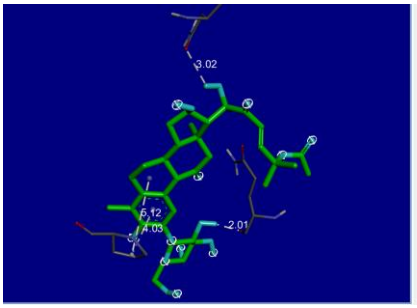

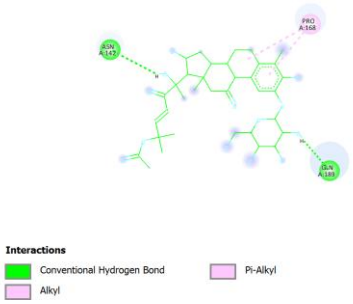

Fevicordin A glucoside (k)

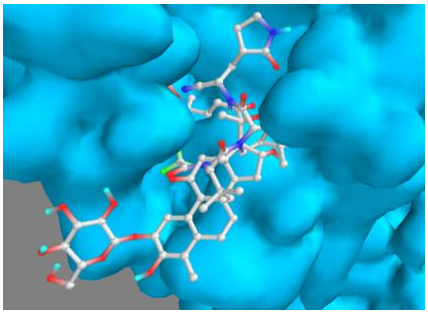

Super imposition of paxlovid and fevicordin A glucoside (k)

Fig. 14. 2D and 3D visualization of molecular interactions between SARS- CoV-2 main protease and Fevicordin A glucoside

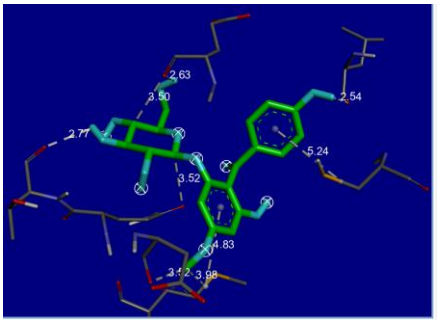

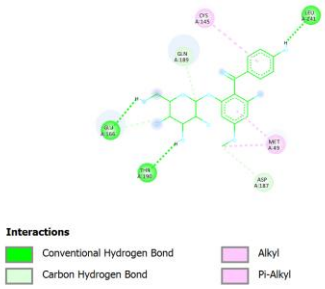

Mahkoside A (l)

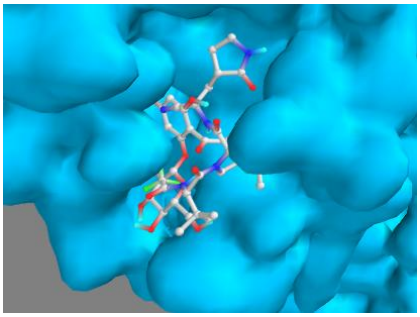

Super imposition of paxlovid and mahkoside A (l)

Fig. 15. 2D and 3D visualization of molecular interactions between SARS- CoV-2 main protease and Mahkoside A

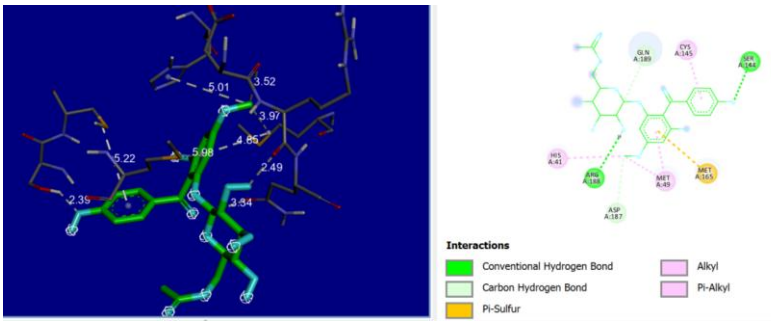

Mahkoside B (m)

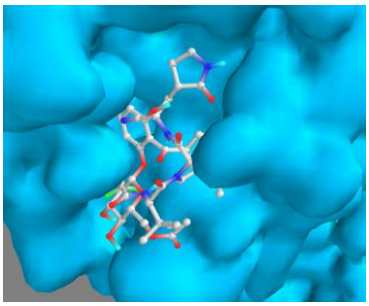

Super imposition of paxlovid and mahkoside B (m)

Fig. 16. 2D and 3D visualization of molecular interactions between SARS- CoV-2 main protease and Mahkoside B

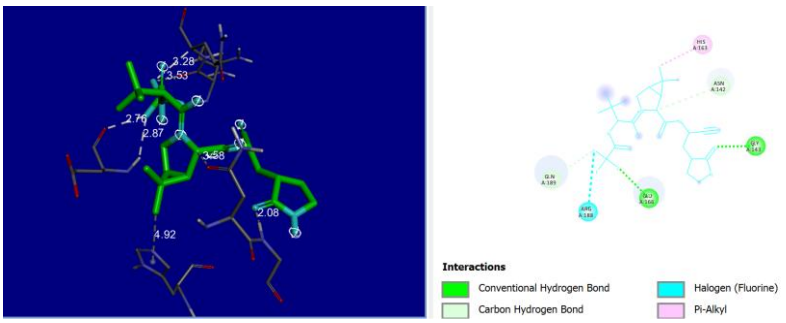

Paxlovid (n)

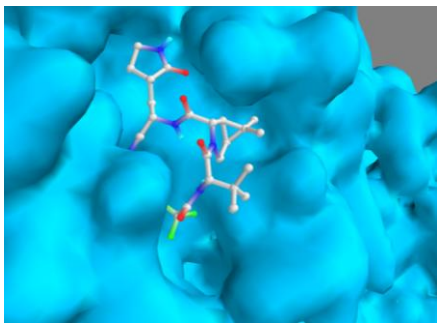

Position of paxlovid on 6LU7 active site (n)

Fig. 17. 2D and 3D visualization of molecular interactions between SARS- CoV-2 main protease

4. CONCLUSION

In summary, molecular docking studies of thirteen phytochemicals from *P.macrocarpa*, also known as mahkota dewa, with the SARS-CoV-2 main protease indicated that some compounds exhibit favourable binding affinity to the protease than the reference molecule, Paxlovid. The molecular interactions of Mahkoside A and Mahkoside B with the main protease of SARS-CoV-2 revealed both compounds interacted with GLN189A, while sesamin interacted with GLU166A. The binding score for each compound is -7.4, - 7.5 and -7.8 kcal/mol respectively. Although these interactions suggest potential relevance to protease binding, the findings should be interpreted as preliminary, as molecular docking alone does not confirm inhibitory activity. Rather than being considered confirmed inhibitors, compounds such as sesamin and mangiferin may be regarded as promising lead compounds or molecular scaffolds for further optimization in antiviral drug development targeting the SARS-CoV-2 main protease.

Due to limitations in GC–MS analysis, several targeted phytochemicals, including quercetin, kaempferol, myricetin, naringenin, gallic acid, sesamin, mangiferin, and others, were not detected. Instead, squalene was identified for its antiviral properties based on the previous study. Thus, squalene was added for in silico docking analysis, but the result shows it is not comparable to sesamin. Besides that, phytochemical screening test that was performed on five compound groups which are flavonoids, terpenoids, phenolics, sterols, and glycosides yielded positive results.

Overall, sesamin was identified as a promising candidate based on the *in silico* docking analysis. SwissADME predictions further suggested favorable pharmacokinetic properties, including high gastrointestinal absorption, blood–brain barrier permeability, compliance with Lipinski's rule, and other drug-likeness criteria. However, this study is limited by its reliance on in silico docking analyses and the lack of experimental validation through in vitro or in vivo studies.

ACKNOWLEDGEMENT

The authors extend their gratitude to Universiti Teknologi MARA for the funding with grant No. 600-RMC-5/3/GPM (038/2023).

REFERENCES

[1] Jinoni, D. A., Benjamin, M. A. Z., Mus, A. A., Goh, L. P. W., Rusdi, N. A., & Awang, M. A. (2024). Phaleria macrocarpa (Scheff.) Boerl. (Mahkota Dewa) seed essential oils: Extraction yield, volatile components, antibacterial, and antioxidant activities based on different solvents using Soxhlet extraction. *Kuwait Journal of Science, 51*(2), 100173. doi: https://doi.org/10.1016/j.kjs.2023.100173

[2] Rahman, F., Tabrez, S., Ali, R., Alqahtani, A. S., Ahmed, M. Z., & Rub, A. (2021). Molecular docking analysis of rutin reveals possible inhibition of SARS-CoV-2 vital proteins. *Journal of Traditional and Complementary Medicine, 11*(2), 173–179. doi: https://doi.org/10.1016/j.jtcme.2021.01.006

[3] Easmin, Mst. S., Sarker, Md. Z. I., Ferdosh, S., Shamsudin, S. H., Yunus, K. bin, Uddin, Md. S., Sarker, Md. M. R., Akanda, Md. J. H., Hossain, Md. S., & Khalil, H. A. (2014). Bioactive compounds and

advanced processing technology: Phaleria macrocarpa (sheff.) Boerl, a review. *Journal of Chemical Technology & Biotechnology, 90*(6), 981–991. doi: https://doi.org/10.1002/jctb.4603

[4] Celia Radita, D., & Widyarman, A. S. (2019). Mahkota Dewa (God's Crown) Fruit Extract Inhibits the Formation of Periodontal Pathogen Biofilms in vitro. *Journal of Indonesian Dental Association, 2*(2), 57. doi: https://doi.org/10.32793/jida.v2i2.404

[5] Agu, P. C., Afiukwa, C. A., Orji, O. U., Ezeh, E. M., Ofoke, I. H., Ogbu, C. O., Ugwuja, E. I., & Aja, P. M. (2023). Molecular docking as a tool for the discovery of molecular targets of nutraceuticals in diseases management. *Scientific Reports, 13*(1), 13398. doi: https://doi.org/10.1038/s41598-023-40160-2

[6] Andrean, D., Prasetyo, S., Kristijarti, A. P., & Hudaya, T. (2014). The Extraction and Activity Test of Bioactive Compounds in Phaleria Macrocarpa as Antioxidants. *Procedia Chemistry, 9,* 94–101. doi: https://doi.org/10.1016/j.proche.2014.05.012

[7] Christy Gnana Theeba P. & Sasi Kumar R.(2015). Phytochemical examination, antioxidant potential and in vitro antibacterial studies of crude extracts of Parthenium hysterophorus Linn. leavesPhytochemical examination, antioxidant potential and in vitro antibacterial studies of crude extracts of Parthenium hysterophorus Linn. Leaves. *Journal of Chemical and Pharmaceutical Research, 2015, 7(4)*:219-225

[8] Godlewska, K., Pacyga, P., Najda, A., & Michalak, I. (2023). Investigation of Chemical Constituents and Antioxidant Activity of Biologically Active Plant-Derived Natural Products. *Molecules, 28*(14), 5572. doi: https://doi.org/10.3390/molecules28145572

[9] Dahanayake, J. M., Perera, P. K., Galappatty, P., Melshandi Perera, H. D. S., & Arawwawala, L. D. A. M. (2019). Comparative Phytochemical Analysis and Antioxidant Activities of Tamalakyadi Decoction with Its Modified Dosage Forms. *Evidence-Based Complementary and Alternative Medicine, 2019*, 1–9. doi: https://doi.org/10.1155/2019/6037137

[10] Deshmukh, M. A., & Theng, M. A. (2018). Phytochemical Screening, Quantitative Analysis Of Primary And Secondary Metabolites Of Acacia Arabica Bark. *International Journal of Current Pharmaceutical Research, 10*(2), 35. doi: https://doi.org/10.22159/ijcpr.2018v10i2.25889

[11] Aqeel, M. T., Nisar-Ur-Rahman, Khan, A., Ashraf, Z., Khan, S., & Arif, M. (2022). In silico approach for the development of phenolic derivatives as potential anti-angiogenic agents against lysyl oxidase-like 2 enzyme. *Future Journal of Pharmaceutical Sciences, 8*(1), 32. doi: https://doi.org/10.1186/s43094-022-00422-8

[12] Boopathi, V., Nahar, J., Murugesan, M., Subramaniyam, S., Kong, B. M., Choi, S.-K., Lee, C.-S., Ling, L., Yang, D. U., Yang, D. C., Mathiyalagan, R., & Chan Kang, S. (2023). In silico and in vitro inhibition of host-based viral entry targets and cytokine storm in COVID-19 by ginsenoside compound K. *Heliyon, 9*(9), e19341. doi: https://doi.org/10.1016/j.heliyon.2023.e19341

[13] Adedayo, A., & Famuti, A. (2023). In-silico studies of Momordica charantia extracts as potential candidates against SARS-CoV-2 targeting human main protease enzyme (Mpro). *Informatics in Medicine Unlocked, 38*, 101216. doi: https://doi.org/10.1016/j.imu.2023.101216

[14] Ebrahimi, M., Farhadian, N., Amiri, A. R., Hataminia, F., Soflaei, S. S., & Karimi, M. (2022). Evaluating the efficacy of extracted squalene from seed oil in the form of microemulsion for the treatment of COVID-19: A clinical study. *Journal of Medical Virology, 94*(1), 119–130. doi: https://doi.org/10.1002/jmv.27273

[15] Fisher, K. J., Kinsey, R., Mohamath, R., Phan, T., Liang, H., Orr, M. T., Lykins, W. R., Guderian, J. A., Bakken, J., Argilla, D., Ramer-Denisoff, G., Larson, E., Qi, Y., Sivananthan, S., Smolyar, K., Carter, D., Paddon, C. J., & Fox, C. B. (2023). Semi-synthetic terpenoids with differential adjuvant properties as sustainable replacements for shark squalene in vaccine emulsions. *Npj Vaccines, 8*(1), 14. doi: https://doi.org/10.1038/s41541-023-00608-y

[16] Stavenga, D. G., Leertouwer, H. L., Dudek, B., & van der Kooi, C. J. (2021). Coloration of Flowers by Flavonoids and Consequences of pH Dependent Absorption. *Frontiers in Plant Science*, 11. doi: https://doi.org/10.3389/fpls.2020.600124

[17] Ibrahim, Z. Y., Uzairu, A., Shallangwa, G. A., & Abechi, S. E. (2021). Pharmacokinetic predictions and docking studies of substituted aryl amine- based triazolopyrimidine designed inhibitors of Plasmodium falciparum dihydroorotate dehydrogenase (PfDHODH). *Future Journal of Pharmaceutical Sciences, 7*(1), 133. doi: https://doi.org/10.1186/s43094-021-00288-2

[18] Tue-ngeun, P., Rakitikul, W., Thinkumrob, N., Hannongbua, S., Meelua, W., & Jitonnom, J. (2024). Binding interactions and in silico ADME prediction of isoconessimine derivatives as potent acetylcholinesterase inhibitors. *Journal of Molecular Graphics and Modelling, 129*, 108746. doi: https://doi.org/10.1016/j.jmgm.2024.108746

[19] Kenny, P. (2022). *Hydrogen bond donors in drug design.* doi: https://doi.org/10.1021/acs.jmedchem.2c01147

[20] Lina Agustin, S., Widiandani, T., Hardjono, S., & Tri Purwanto, B. (2022). QSAR of Acyl pinostrobin derivatives as Anti-breast cancer against HER-2 receptor and their ADMET properties based on in silico Study. *Research Journal of Pharmacy and Technology*, 4641 doi: https://doi.org/10.52711/0974-360x.2022.00779

[21] Miebs, G., Mielniczuk, A., Kadziński, M., & Bachorz, R. A. (2024). Beyond the Arbitrariness of Drug-Likeness Rules: Rough Set Theory and Decision Rules in the Service of Drug Design. *Applied Sciences, 14*(21), 9966. doi: https://doi.org/10.3390/app14219966

[22] Babalola, B. A., & Adegboyega, A. E. (2024). Computational Discovery of Novel Imidazole Derivatives as Inhibitors of SARS-CoV-2 Main Protease: An Integrated Approach Combining Molecular Dynamics and Binding AffinityAnalysis. *COVID, 4*(6), 672–695. doi: https://doi.org/10.3390/covid4060046

[23] Gangadhar Y, Al Turaifi AR, Naveen NR, Goudanavar P, Fattepur S, et al. Bio-Simulation Studies of Valganciclovir Hydrochloride: Molecular Descriptor-Based QSAR Modelling and Swiss ADME Analysis Using in silico Models. Indian J of Pharmaceutical Education and Research. 2025;59(1):1-10 doi: https://doi.org/10.5530/ijper.20251137

[24] Price, G., & Patel, D. A. (2025). Drug Bioavailability. National Library of Medicine. StatPearls Publishing LLC. url: https://www.ncbi.nlm.nih.gov/books/NBK557852/

[25] Lin, J. H., & Yamazaki, M. (2003). Role of P-Glycoprotein in Pharmacokinetics. *Clinical Pharmacokinetics, 42*(1), 59–98. doi: https://doi.org/10.2165/00003088-200342010-00003

[26] Huang, L., Li, B., Li, X., Liu, G., Liu, R., Guo, J., Xu, B., Li, Y., & Fang, W. (2019). Significance and Mechanisms of P-glycoprotein in Central Nervous System Diseases. *Current Drug Targets, 20*(11), 1141–1155. doi: https://doi.org/10.2174/1389450120666190308144448

[27] Nur Hannani Ahmad Rozani, Fatahiya Mohamed Tap, Fadzilah Adibah Abd Majid, Nur 'Ainun Mokhtar, & Nurul Bahiyah Ahmad Khairudin. (2024). Molecular Docking of Phytochemicals from M. Charantia Targeting SARS- CoV-2 Main Protease. *Journal of Advanced Research in Applied Sciences and Engineering Technology, 47*(1), 152–165. doi: https://doi.org/10.37934/araset.47.1.152165

[28] Amelia, M. A., Kesuma, D., Kirtishanti, A., Sumartha, I. G. A., & Claudya, M. (2024). Molecular Docking: Study of Chalcone Derivatives from Boesenbergia pandurata Targeting Estrogen Receptor Alpha (ER–a) for Breast Cancer. *Jurnal Penelitian Pendidikan IPA, 10*(11), 8376–8386. doi: https://doi.org/10.29303/jppipa.v10i11.8734

[29] Akhtar, N., Verma, H., Silkari, O. M., Upadhyay, A. K., Kaushik, V., & Amin-ul Mannan, M. (2022). Drummondin E and Flinderole B are potential inhibitors of RNA-dependent RNA polymerase of SARS-CoV-2: an in silico study. *BioTechnologia, 103*(1), 53–70. doi: https://doi.org/10.5114/bta.2022.113915

[30] Kawsar, S. M. A., Hosen, M. A., el Bakri, Y., Ahmad, S., Affi, S. T., & Goumri- Said, S. (2022). In silico approach for potential antimicrobial agents through antiviral, molecular docking, molecular dynamics, pharmacokinetic and bioactivity predictions of galactopyranoside derivatives. *Arab Journal of Basic and Applied Sciences, 29*(1), 99–112. doi: https://doi.org/10.1080/25765299.2022.2068275

[31] Harisna, A. H., Nurdiansyah, R., Syaifie, P. H., Nugroho, D. W., Saputro, K. E., Firdayani, Prakoso, C. D., Rochman, N. T., Maulana, N. N., Noviyanto, A., & Mardliyati, E. (2021). In silico investigation of potential inhibitors to main protease and spike protein of SARS-CoV-2 in propolis. *Biochemistry and Biophysics Reports, 26*, 100969. doi: https://doi.org/10.1016/j.bbrep.2021.100969

[32] Zhu, M., Pan, J., Hu, X., & Zhang, G. (2021). Epicatechin Gallate as Xanthine Oxidase Inhibitor: Inhibitory Kinetics, Binding Characteristics, Synergistic Inhibition, and Action Mechanism. *Foods, 10*(9), 2191. doi: https://doi.org/10.3390/foods10092191